Published in final edited form as:
Graefes Arch Clin Exp Ophthalmol. 2012 March ; 250(3): 349–359. doi:10.1007/s00417-011-1856-9.

Proteomic profiling of human retinal pigment epithelium exposed to an advanced glycation-modified substrate

J. V. Glenn,
School of Medicine, Dentistry and Biomedical Science, Queen's University Belfast, Northern Ireland, UK

H. Mahaffy,
School of Medicine, Dentistry and Biomedical Science, Queen's University Belfast, Northern Ireland, UK

S. Dasari,
School of Medicine, Dentistry and Biomedical Science, Queen's University Belfast, Northern Ireland, UK

M. Oliver,
Waters MS Technology Centre, Atlas Park, Manchester, UK

M. Chen,
School of Medicine, Dentistry and Biomedical Science, Queen's University Belfast, Northern Ireland, UK

M. E. Boulton,
Department of Anatomy and Cell Biology, University of Florida, Gainesville, FL, USA

H. Xu,
School of Medicine, Dentistry and Biomedical Science, Queen's University Belfast, Northern Ireland, UK

W. J. Curry, and
School of Medicine, Dentistry and Biomedical Science, Queen's University Belfast, Northern Ireland, UK

Alan W. Stitt
School of Medicine, Dentistry and Biomedical Science, Queen's University Belfast, Northern Ireland, UK

Abstract

Purpose—The retinal pigment epithelium (RPE) and underlying Bruch's membrane undergo significant modulation during ageing. Progressive, age-related modifications of lipids and proteins by advanced glycation end products (AGEs) at this cell–substrate interface have been implicated in RPE dysfunction and the progression to age-related macular degeneration (AMD). The pathogenic nature of these adducts in Bruch's membrane and their influence on the overlying RPE remains unclear. This study aimed to identify alterations in RPE protein expression in cells

A. W. Stitt (✉) Centre for Vision and Vascular Science, Queen's University Belfast, Royal Victoria Hospital, Belfast, BT12 6BA Northern Ireland, UK a.stitt@qub.ac.uk.

J.V. Glenn and H. Mahaffy contributed equally to the research

None of the authors have conflicts of interest or requirement for financial disclosure.

exposed to AGE-modified basement membrane (AGE-BM), to determine how this “aged” substrate impacts RPE function and to map the localisation of identified proteins in ageing retina.

Methods—Confluent ARPE-19 monolayers were cultured on AGE-BM and native, non-modified BM (BM). Following 28-day incubation, the proteome was profiled using 2-dimensional gel electrophoresis (2D), densitometry and image analysis was employed to map proteins of interest that were identified by electrospray ionisation mass spectrometry (ESI MS/MS). Immunocytochemistry was employed to localise identified proteins in ARPE-19 monolayers cultured on unmodified and AGE-BM and to analyze aged human retina.

Results—Image analysis detected altered protein spot densities between treatment groups, and proteins of interest were identified by LC ESI MS/MS which included heat-shock proteins, cytoskeletal and metabolic regulators. Immunocytochemistry revealed deubiquitinating enzyme ubiquitin carboxyterminal hydrolase-1 (UCH-L1), which was upregulated in AGE-exposed RPE and was also localised to RPE in human retinal sections.

Conclusions—This study has demonstrated that AGE-modification of basement membrane alters the RPE proteome. Many proteins are changed in this ageing model, including UCHL-1, which could impact upon RPE degradative capacity. Accumulation of AGEs at Bruch”s membrane could play a significant role in age-related dysfunction of the RPE.

Keywords

Bruch’s membrane; RPE; Advanced glycation endproducts; Ubiquitin carboxyterminal hydrolase-1

Introduction

The retinal pigment epithelium (RPE) plays a key role in retinal function by transferring retinoids to the photoreceptor layer as part of the visual cycle, phagocytosing spent photoreceptor outer segments and acting as a selective filtration barrier between the dense vascular network of the choriocapillaris and the RPE. At this interface, the RPE rests on Bruch’s membrane, and this complex pentalaminar matrix plays a critical role in RPE function and maintenance of outer retinal integrity [1].

During ageing, Bruch’s membrane undergoes a series of structural and physiological changes that increase its thickness and induce an ill-defined re-configuration of its chemical composition [2, 3]. Crosslinking of component collagens and decreased solubility with age [4] occur in unison with the accumulation of granular, membranous, filamentous, and vesicular material, and characteristic changes in membrane lipid composition [5]. Human Bruch’s membrane lipid content increases throughout life [6], and an exponential age-related increase in phospholipids, triglycerides, fatty acids, and free cholesterol content has been reported [7]. These changes are linked to the development of various forms of extracellular material, termed drusen, that can alter RPE function and serve as a precursor of age-related maculopathy (ARM) and progression to age-related macular degeneration (AMD) [8]. AMD is a degenerative retinal disorder characterised by sub-RPE drusen deposition, lipofuscin accumulation, RPE cell death and subsequent choroidal neovascularisation. AMD constitutes the leading cause of blindness in Western societies, yet its precise pathogenesis is uncertain, and therapeutic options for treating the variant forms of AMD remain severely limited [1].

Studies suggest that lipid and protein modification by Maillard chemistry during the ageing process leads to significant accumulation of AGEs at the Bruch’s membrane–RPE axis [9–13]. AGEs form from the reaction of ε–amino groups with glucose, lipid peroxidation

products, or various α-oxaloaldehydes; they accumulate principally, but not exclusively, on long-lived structural proteins such as collagens and lens crystallins [14], and may act as important pathogenic agents in age-related pathology by causing crosslinking, altering protein interactions, and inducing pro-oxidant/pro-inflammatory AGE-receptor signalling in cells [10, 15–18]. AGE concentrations are elevated in RPE, drusen, and Bruch's membrane from aged human eyes [19, 20], especially those with AMD [9–12]. AGE crosslinks on the RPE substrate are known to have impact on the photoreceptor outersegment degradative function of these cells, and this causes significantly enhanced lipofuscin accumulation [21]. The potential pathogenic impact that Bruch's membrane-immobilized AGEs have on the RPE requires further investigation. The current investigation utilised a well-characterised AGE-modified substrate to examine its impact on RPE proteome and to begin to characterise the putative pathogenic role for these adducts in age-related dysfunction.

Materials and methods

RPE culture and preparation of AGE-modified BM

The human ARPE-19 cell line, obtained from ATCC (Rockville, MD, USA), was maintained as detailed previously [21]. RPE substrate was prepared according to a method outlined by Stitt et al. [22], in which Matrigel™ BM extract (Becton Dickinson, Oxford, UK) was AGE-modified to mimic ageing of the innermost face of Bruch's membrane. Briefly, non-modified Matrigel™ was designated control BM, while AGE-modification was induced by exposure to glycolaldehyde (Sigma-Aldrich Company Ltd., Dorset, UK) (50–200 mM in PBS) for 4 hr at 37°C. The degree of AGE modification and crosslinking on this model substrate has been previously described [22].

Protein extraction and 2-dimensional gel electrophoresis (2DGE)

ARPE-19 cells were plated onto unmodified native BM or AGE-BM substrates and maintained for 1 month in medium supplemented with 2% (v/v) foetal calf serum (FCS). RPE monolayer cultures were extracted in ice-cold PBS, centrifuged (13,000×g, 15 min) and dialyzed using Slide-A-Lyzer cassettes (3500 kDa, Pierce, Rockford, IL, USA); the dialyzate was lyophilised to aid protein concentration, and samples were reconstituted in 2D rehydration buffer (8 M urea, 2% CHAPS w/v) and protein content determined (2D-Quant kit, Amersham Biosciences Ltd., Buckinghamshire, UK).

Extracts were standardised to 450 μl (2 mg protein) in immobilised pH gradient (IPG) buffer in the relevant pH range. IPG strips (IPG, 18 cm, pH 3–10 and 4–7 NL: Amersham Biosciences Ltd., Buckinghamshire, UK) were rehydrated for 18 hours and isoelectric focusing (IEF) performed. Strips were placed on precast bisacrylamide gels (dimensions of 255 × 196 × 1 mm) and SDS-PAGE (12.5%) performed using the Ettan DALTsix vertical system (Amersham Biosciences Ltd., Buckinghamshire, UK), with gels electrophoresed at 600 V for 30 min, then 600 V for 4 hours. Colloidal Coomassie Blue (Sigma-Aldrich Company Ltd., Dorset, UK) was routinely used to visualise protein spots.

The gels were scanned using a GS-800 calibrated densitometer (Bio-Rad Laboratories Inc., Hercules, CA, USA) and image analysis was performed using Progenesis PG220 (Nonlinear Dynamics Ltd., Newcastle upon Tyne, UK). Gels were imported, and spot detection and matching was performed automatically in Progenesis, followed by manual adjustment to correct for potential differences in protein loading between gels, as previously described [23]. To analyse protein expression changes, only filtered spots exceeding an intensity threshold of 1.5- to 2-fold increase or decrease between the two ages were subjected to further analysis; the threshold regulation factor for the significance level was set at $p \leq 0.05$. Spots altered beyond the factor required for significance were considered as candidate spots,

and subsequently subjected to manual verification. Spots displaying significant expression changes were subsequently identified by MS.

Protein spot identification by mass spectrometry (MS)

Protein spots of interest were excised, washed and destained until all Coomassie Blue was removed. Gel spots were dehydrated in 25 μl acetonitrile at room temperature, dried in a HT-4 series II centrifugal evaporator (GeneVac Ltd., Ipswich, UK) for 30 min and subjected to tryptic digestion (Promega Corporation, Madison, WI, USA) to extract peptide fragments. Following tryptic digestion, 30 μl 5% (v/v) trifluoroacetic acid (TFA), 50% (v/v) acetonitrile in deionised H_2O was added to the samples to extract the peptide fragments prior to lyophilisation.

Liquid chromatography electrospray tandem mass spectrometry (LC-ESI-MS/MS) was completed at Micromass (Waters Ltd., Manchester, UK). The dried digested proteins were analysed by LC-ESI-MS/MS using a Waters Micromass modular CapLC connected to the source of a Waters Micromass Q-TOF Ultima API tandem mass spectrometer, as described previously [24]. Mass spectra and tandem mass spectra were analysed using the Applied Biosystems GPS Explorer (Applied Biosystems, Foster City, CA, USA). Sequence tag searches and protein identifications were completed using an in-house MASCOT server searching against the Swiss-Protein and NCBI protein sequence databases.

Immunocytochemistry & immunoblotting of RPE cell monolayers

ARPE-19 cells were cultured as described above for a period of 4 weeks post confluency. Monolayers were fixed in 4% PFA prior to blocking and permeabilisation (PBS-Tween [PBS-T], 0.1% and 5% normal goat serum [NGS]). UCH-L1/protein gene product 9.5 murine monoclonal antibody (1/1400 dilution) (Chemicon, Millipore, UK) was incubated overnight at 4°C. After incubation with primary antibody, cells were washed with PBS-T (5×5 min) prior to incubation with Alexa 488 goat anti mouse IgG conjugated secondary antibody (Molecular Probes, Invitrogen, UK) for 1 hr at room temperature. Sections were washed with PBS-T and mounted in mounting medium with propidium iodide (PI) to preserve fluorescence and counterstain DNA (Vector Laboratories, Burlingame, CA, USA) (as above), and viewed by fluorescent microscopy and images recorded by the Lucia GF imaging system (Nikon, Surrey, UK).

Cell extracts were prepared by scraping whole cell monolayers into RIPA buffer, followed by overnight rotary extraction at 4°C followed by removal of supernatant. Total protein was determined in the supernatants by BCA analysis (Pierce, MSC, Eire). Twenty microgram protein samples were heated in loading buffer (Invitrogen, Paisley, UK), 95°C, 5 mins and allowed to cool before loading for electrophoresis.

Electrophoresis was performed as described above using 12% polyacrylamide gel electrophoresis, followed by transfer to Immobilon-P polyvinylidene fluoride (PVDF) membrane (Millipore, UK). Membranes were washed with PBST (0.1%) and incubated overnight at 4°C in PBST containing 4% (w/v) Blotto milk protein (Santa Cruz Biotechnology, Santa Cruz, CA, USA) to block nonspecific reactivity, followed by washing and incubation in UCH-L1/protein gene product 9.5 murine primary monoclonal antibody (1/1000 dilution in PBST) (Chemicon, Millipore, UK) overnight at 4°C. A commercial fluorescent secondary antibody (IRDye 800CW goat-anti mouse IgG) was added (1/5000 dilution) and membranes imaged using the Odyssey Infrared imaging system (LI-COR, Biosciences, Future Lab Technologies, Eire). A, β-actin loading control was also analysed with β-actin primary antibody (Sigma-Aldrich) and comparable secondary antibody (IRDye 680 IgG, 1/5000 dilution). Fluorescence density for UCHL-1 and β-actin was analysed

simultaneously using the LI-COR band quantification system, which provides a broad, linear dynamic range of fluorescence intensity, unlike conventional chemiluminescence which is dependent on timing and exposure, and is restricted to a defined linear range.

Localisation of UCH-L1 in human retina

All methods were carried out in accordance with the tenets of the Declaration of Helsinki for any research involving human tissue. In addition, informed consent was obtained from relatives prior to the study, and ethical approval was obtained from Research Ethics Committees of all involved Institutions. Eyecups were retrieved approximately 4 hours post-mortem and immediately placed on ice. The anterior portion of the eye was removed and the retina immersion fixed in 4% PFA (Sigma-Aldrich Company Ltd., Dorset, UK) for 1 hr at room temperature. After paraffin embedding, tissue sections (7 μm) were cut and placed upon silanized slides and allowed to air-dry before use.

Seven-μm sections were deparaffinised in xylene (3×5 min), followed by rehydration in 100%, 95%, 70% (v/v) ethanol/H_20, and distilled H_2O. Sections were blocked and placed in permeabilisation buffer (PBS-Tween [PBS-T], 0.1% and 5% NGS) prior to incubation with UCH-L1 monoclonal antibody (1/2000 dilution) [Chemicon (protein gene product 9.5), Millipore, UK] 18 hr, 4^0 C. Sections were washed in PBS-T (5×5 min) prior to incubation with Alexa 488 goat anti-mouse IgG conjugated secondary antibody (Molecular Probes, Invitrogen, UK) for 1 hr at room temperature. Sections were washed (PBS-T) and mounted as described above for monolayer ICC. Samples were viewed by fluorescent microscopy and images recorded by both confocal microscopy and the Lucia GF system. In all cases, isotype controls consisting of nonimmune sera were employed (Sigma Aldrich, UK).

Statistical analysis

Data were expressed as the mean values ± SEM, and statistical differences in the mean were assessed using one-way analysis of variance (ANOVA) followed by the Tukey–Kramer post-hoc test for multiple comparisons unless stated specifically. All statistical analyses were performed using SPSS 14.0 (Lead Technologies, USA) or GraphPad InStat 3.0 (GraphPad Software, San Diego, CA, USA). Data was considered significant at 95% ($p<0.05$).

Results

Proteins identified by 2D-SDS-PAGE (pH range 3–10)

The proteomes for ARPE-19 cultured for 1 month on unmodified BM (control) and AGE-BM were profiled. In the first instance, extracted protein was resolved using IEF pH 3–10 in the first dimension, and arrayed using a 12.5 % gel (Fig. 1) ($n=3$); 322 ± 25 spots following culture with native BM compared relative to 235 ± 10 spots following culture on AGE-BM ($n=3$). Nineteen protein spots were identified by LC ESI–MS/MS from the control RPE (Fig. 1a), and 15 proteins from RPE exposed to AGE-BM for 1 month (Table 1; Fig. 1b).

Proteins identified by 2D-SDS-PAGE (pH range 4–7)

RPE proteins were resolved using a linear pH range (pH 4–7) in the first dimension (Fig. 2); ($n=3$). 2D-PAGE detected 279 ± 16 and 221 ± 37 from RPE cells cultured on BM and AGE-BM respectively. Proteins of interest from RPE cultured on control substrate were analysed by ESI-MS/MS (Fig. 2a) and 31 identified (Table 1), while 37 spots from RPE cultured on AGE-BM were identified (Fig. 2b).

Densitometry detected altered spot densities for several matched proteins, some of which were identified by ESI-MS/MS (Tables 1, 2, Fig. 3). Incubation of the RPE on AGE-BM

induced a 2.1- and 4.5-fold increase in protein disulphide isomerase (PDI) and ubiquitin carboxyl-terminal hydrolase 1 (UCH L1) densitometry respectively. In addition, a number of RPE proteins exhibited decreased expression when cultured on AGE-BM; these included phosphoglycerate kinase (8.4-fold), c myc promoter binding protein (4.9-fold), and tumour necrosis factor beta (TNF-β) precursor (5.9-fold).

Analysis of the identified spots demonstrated that the majority of proteins belong to specific groups with specialised functions; the largest number of alterations were evident in heat-shock proteins, cytoskeletal proteins, and those linked to metabolic regulation (Table 2).

Localisation and regulation of UCH-L1 in human RPE

AGE-exposure induced a 4.5-fold increase in the proteasome-linked protein UCH-L1, and this was corroborated with complementary immunocytochemistry analysis. Confluent RPE monolayers cultured for 1 month on native BM substrate revealed moderate cytoplasmic UCH-L1 immunoreactivity. The relative intensity increased when cells were grown on AGE-BM (Fig. 4). Western blot analysis of RPE extracts confirmed upregulation of protein UCH-L1 in cell monolayers cultured upon AGE-BM relative to control RPE on BM ($p<0.05$) (Fig. 4c,d).

Immunohistochemical analysis of aged human ocular tissues ($n=7$) revealed the expression of UCH-L1 in the outer retina, where it was predominantly localised to the RPE (Fig. 5). In the older donor tissue, there was a qualitative increase in UCH-L1 protein in the RPE.

Discussion

A normal human RPE proteomic database was established in 2003 [25], and since then the proteomes derived from RPE recovered from aged donor eyes and cultured ARPE-19 cells have been reported [26–29]. As denoted in Table 1, many of the regulated proteins observed in the current analysis have also been demonstrated in other RPE proteomes. Most of these studies have identified age-related alterations in key component proteins in metabolic pathways such as the MAPK (mitogen-activated protein kinase) cascade, lysosomal cathepsins, and stress responses markers [9, 30]. Several studies have also evaluated the mechanisms of RPE activation under oxidative stress, ageing, disease states, and normal growth [31] [26–28, 30, 32–34]. The current investigation employed a model of aged Bruch's membrane to assess its impact on the RPE proteome. The densities of several identified protein spots were increased following exposure to AGEs in the sub-cellular matrix, many of which have a significant role in degradative RPE pathways, such as the deubiquiting enzyme UCH-L1, proactivator polypeptide precursor (involved in lysosomal degradation of sphingolipids), and nucleophosmin (a histone chaperone protein). Additional identified proteins have antioxidant functions, such as the thioredoxin-dependent peroxide, peroxiredoxin 2, and protein disulphide isomerase that are involved in regulating redox potential.

The majority of the proteins that exhibited decreased detection when cultured on AGE-BM are involved in glycolysis/gluconeogenesis, such as phosphoglycerate kinase (a glycolytic transferase enzyme), c-myc promoter binding protein (an inhibitor of MAPK pathway), triosephosphate isomerase (catalysis of triose phosphates isomers), and inflammation mediator tumour necrosis factor β precursor. Several other proteins identified by MS/MS, such as cathepsin D precursor protein, alpha and gamma enolase, superoxide dismutase, galectin-1, and the structural proteins myosin and actin did not exhibit statistical significance for altered expression.

Structural integrity proteins

The identification of the intermediate filament protein vimentin in RPE was not surprising, since it is a key cytoskeletal component in these cells. However, its upregulation in the RPE after exposure to AGE-BM was interesting, since increased vimentin expression has been confirmed in RPE from AMD patients [35]. This observation lends support to the concept that in some respects age-related changes in vitro may parallel those observed in vivo in terms of initial phenotypic variation [19, 21]. Vimentin has been reported as a major target for specific AGE modification in dermal fibroblasts, in which the majority of glycation events were evident on lysine residues located in linker regions [36]. This non-random AGE modification induced a redistribution of vimentin to form perinuclear aggregates, induced decreased contractility, and the CML-modified vimentin accumulated and evidently drove aggresome formation [36]. This association strongly supports the concept that AGE modifications generate loss of function. The functional significance of increased vimentin detection in RPE cultured on AGE-BM warrants further detailed analysis to assess gene expression and protein turnover.

Calmodulin exhibited increased detection in RPE exposed to AGE-BM, and this could be related to impaired adhesion of the cells through impaired matrix interaction. This protein is a multifunctional cytoplasmic calcium-binding receptor which has diverse functions in multiple cell types in which it binds to other proteins [37]. In the context of the RPE, it may play a role in proliferative vitreoretinopathy (PVR) in which RPE hyperproliferation leads to development of epiretinal membranes [38]. Indeed, calcium and calmodulin antagonists have been shown to reduce RPE proliferation, and have been discussed as potential PVR therapies [39]. The present study detected increased RPE calmodulin densities in response to growth on AGE-BM

Markers of apoptosis/stress response elements

α-crystallin was not detected in RPE cultured on AGE-BM, and this would suggest that either protein expression was significantly downregulated and/or it is subject to unknown posttranslational modification [40], which may impact its solubility and migration. Increased oxidative stress has been reported to downregulate α crystallin mRNA expression, and this stressor is characteristic of RPE cultured on a glycated matrix [41, 42]. α crystallin is subjected to considerable modification with ageing [43], but it is uncertain if AGE adducts in the sub-cellular matrix could have any impact on intracellular AGE formation.

Protein disulphide isomerase (PDI) is expressed by quiescent RPE in vitro [25], where it may act as a chaperone and as a catalyst for disulphide bond formation [44]. The current study detected elevated PDI levels in RPE cultured on AGE-BM, and several studies have established that mRNA and protein PDI expression is upregulated in response to cellular oxidative or hypoxic stress [40, 45, 46]. Therefore, since it is well-documented that AGEs induce oxidative stress, it is reasonable to suggest that prolonged RPE exposure to AGE-BM could lead to an increased oxidative burden and a concomitant increase in PDI expression.

The current study detected decreased density of heat shock protein (HSP) following AGE-exposure. HSP have recently been shown to be involved in defence against oxidative stress in AMD retina/RPE [47] and upregulated in response to high glucose conditions [32]. HSPs have been linked to caspase activation and apoptotic responses [48, 49].

Alteration in ubiquitin carboxyl-terminal hydrolase 1 (UCH-L1)

The ubiquitin proteasome pathway (UPP) is essential for specific, regulated degradation and removal of ubiquitinated proteins [50]. UCH-L1, a thiol (cysteine) protease, is a member of the ubiquitin carboxyl-terminal hydrolase (UCH) family of deubiquitinating enzymes

(DUBs). UCH-L1 is expressed in neural tissue, and occurs at elevated concentrations in aggregates characteristic of neurodegeneration diseases such as Lewy bodies (Parkinson's disease) and neurofibrillary tangles (Alzheimer's disease) [51–53]. UCH-L1 has been localised to retinal ganglion cells; cells in the inner nuclear layer and in neuronal fibers in the plexiform layers [54] and in RPE cells [55]. UCH-L1 exhibited increased detection both in vitro and in vivo in human retina, and more intense immunostaining was observed in the photoreceptor outer segments of aged mice in particular, at the RPE/photoreceptor interface. Previous reports have also shown localisation of UCH-L1 to the inner segments of cones [55]. This suggests a close association with ubiquitin deposition and the localisation of the ubiquitin conjugating enzyme E2 [55]. The current study suggests that this enzyme may also be important in RPE function, although further studies would need to examine how it alters in detailed human post-mortem studies.

Age-related protein damage via oxidative stress is a characteristic feature of advanced glycation reactions, and would be expected to place considerable demand on the ubiquitin system. Previous studies have shown increased accumulation of lipofuscin in a murine mode of retinal ageing, both in subretinal/RPE and perivascular tissues, and associated with increased fundus autofluorescence also linked to potential AGE deposition [56]. This data is supportive of current observation in aged murine and human retina. Proteome analysis of drusen/lipofuscin isolated from AMD patients also detected ubiquitin [57]. This report allied with the current observations would suggest that the ubiquitin system in general and the activity of UCH-L1 in particular are worthy of further study.

Prolonged exposure to an AGE-modified substrate (akin to aged Bruch's membrane) has a significant effect on the RPE proteome in vitro. This study has shown that a range of pathogenic pathways may become dysfunctional upon prolonged exposure of RPE to AGE adducts characteristic of ageing. In particular, this study has highlighted the potential disruption to intracellular protein degradation, which has implications for the health of the outer retina.

Acknowledgments

The authors would like to acknowledge financial support from the Wellcome Trust, The Medical Research Council (MRC), Action Medical Research, and NIH grant EY019688. The authors would like to thank the Bristol Eye Bank for their donation of clinical material. AWS holds a Royal Society Wolfson Merit Award.

Abbreviations

2D	two dimensional gel electrophoresis
AGE-BM	AGE modified basement membrane extract
AGEs	advanced glycation endproducts
AMD	age-related macular degeneration
ARM	age-related maculopathy
DUBs	deubiquitinating enzymes
ESI MS/MS	electrospray ionisation mass spectrometry
FCS	foetal calf serum
HSP	heat shock protein
IEF	isoelectric focusing
IHC	Immunohistochemistry

LC-ESI-MS/	Liquid chromatography electrospray tandem
MS	mass spectrometry
MAPK	mitogen-activated protein kinase
NGS	Normal goat serum
PDI	protein disulphide isomerase
PFA	Paraformaldehyde
PI	propidium iodide
PVDF	polyvinylidene fluoride
PVR	proliferative vitreoretinopathy
RPE	retinal pigment epithelium
TFA	trifluoroacetic acid
TNF-β	tumour necrosis factor beta
BM	unmodified basement membrane extract
UCH	Ubiquitin carboxyl-terminal hydrolase
UCH-L1	Ubiquitin carboxyterminal hydrolase-1
UPP	Ubiquitin proteasome pathway

References

1. Zarbin MA. Current concepts in the pathogenesis of age-related macular degeneration. Arch Ophthalmol. 2004; 122:598–614. [PubMed: 15078679]
2. Curcio CA, Johnson M, Huang JD, Rudolf M. Aging, age-related macular degeneration, and the response-to-retention of apolipoprotein B-containing lipoproteins. Prog Retin Eye Res. 2009; 28:393–422. [PubMed: 19698799]
3. Okubo A, Rosa RH Jr, Bunce CV, Alexander RA, Fan JT, Bird AC, Luthert PJ. The relationships of age changes in retinal pigment epithelium and Bruch's membrane. Invest Ophthalmol Vis Sci. 1999; 40:443–449. [PubMed: 9950604]
4. Karwatowski WS, Jeffries TE, Duance VC, Albon J, Bailey AJ, Easty DL. Preparation of Bruch's membrane and analysis of the age-related changes in the structural collagens. Br J Ophthalmol. 1995; 79:944–952. [PubMed: 7488585]
5. Karwatowski WS, Jeffries TE, Duance VC, Albon J, Bailey AJ, Easty DL. Collagen and ageing in Bruch's membrane. Biochem Soc Trans. 1991; 19:349S. [PubMed: 1794487]
6. Pauleikhoff D, Harper CA, Marshall J, Bird AC. Aging changes in Bruch's membrane. A histochemical and morphologic study. Ophthalmol. 1990; 97:171–178.
7. Sheraidah G, Steinmetz R, Maguire J, Pauleikhoff D, Marshall J, Bird AC. Correlation between lipids extracted from Bruch's membrane and age. Ophthalmol. 1993; 100:47–51.
8. Coffey AJ, Brownstein S. The prevalence of macular drusen in postmortem eyes. Am J Ophthalmol. 1986; 102:164–171. [PubMed: 3740175]
9. Schutt F, Bergmann M, Holz FG, Kopitz J. Proteins modified by malondialdehyde, 4-hydroxynonenal, or advanced glycation end products in lipofuscin of human retinal pigment epithelium. Invest Ophthalmol Vis Sci. 2003; 44:3663–3668. [PubMed: 12882821]
10. Howes KA, Liu Y, Dunaief JL, Milam A, Frederick JM, Marks A, Baehr W. Receptor for advanced glycation end products and age-related macular degeneration. Invest Ophthalmol Vis Sci. 2004; 45:3713–3720. [PubMed: 15452081]

11. Handa JT, Verzijl N, Matsunaga H, Aotaki-Keen A, Lutty GA, te Koppele JM, Miyata T, Hjelmeland LM. Increase in the advanced glycation end product pentosidine in Bruch's membrane with age. Invest Ophthalmol Vis Sci. 1999; 40:775–779. [PubMed: 10067983]
12. Ishibashi T, Murata T, Hangai M, Nagai R, Horiuchi S, Lopez PF, Hinton DR, Ryan SJ. Advanced glycation end products in age-related macular degeneration. Arch Ophthalmol. 1998; 116:1629–1632. [PubMed: 9869793]
13. Yamada Y, Ishibashi K, Bhutto IA, Tian J, Lutty GA, Handa JT. The expression of advanced glycation endproduct receptors in rpe cells associated with basal deposits in human maculas. Exp Eye Res. 2006; 82:840–848. [PubMed: 16364296]
14. Monnier VM, Sell DR, Nagaraj RH, Miyata S, Grandhee S, Odetti P, Ibrahim SA. Maillard reaction-mediated molecular damage to extracellular matrix and other tissue proteins in diabetes, aging, and uremia. Diabetes. 1992; 41(Suppl 2):36–41. [PubMed: 1526333]
15. Ma W, Lee SE, Guo J, Qu W, Hudson BI, Schmidt AM, Barile GR. RAGE ligand upregulation of VEGF secretion in ARPE-19 cells. Invest Ophthalmol Vis Sci. 2007; 48:1355–1361. [PubMed: 17325184]
16. Alves M, Calegari VC, Cunha DA, Saad MJ, Velloso LA, Rocha EM. Increased expression of advanced glycation end-products and their receptor, and activation of nuclear factor kappa-B in lacrimal glands of diabetic rats. Diabetologia. 2005; 48:2675–2681. [PubMed: 16283249]
17. Yamada Y, Ishibashi K, Ishibashi K, Bhutto IA, Tian J, Lutty GA, Handa JT. The expression of advanced glycation end-product receptors in rpe cells associated with basal deposits in human maculas. Exp Eye Res. 2006; 82:840–848. [PubMed: 16364296]
18. Zhou J, Cai B, Jang YP, Pachydaki S, Schmidt AM, Sparrow JR. Mechanisms for the induction of HNE- MDA- and AGE-adducts, RAGE and VEGF in retinal pigment epithelial cells. Exp Eye Res. 2005; 80:567–580. [PubMed: 15781285]
19. Beattie JR, Pawlak AM, Boulton ME, Zhang J, Monnier VM, McGarvey JJ, Stitt AW. Multiplex analysis of age-related protein and lipid modifications in human Bruch's membrane. FASEB J. 2010; 24:4816–4824. [PubMed: 20686107]
20. Glenn JV, Beattie JR, Barrett L, Frizzell N, Thorpe SR, Boulton ME, McGarvey JJ, Stitt AW. Confocal Raman microscopy can quantify advanced glycation end product (AGE) modifications in Bruch's membrane leading to accurate, nondestructive prediction of ocular aging. FASEB J. 2007; 21:3542–3552. [PubMed: 17567569]
21. Glenn JV, Mahaffy H, Wu K, Smith G, Nagai R, Simpson DA, Boulton ME, Stitt AW. Advanced glycation end product (AGE) accumulation on Bruch's membrane: links to age-related RPE dysfunction. Invest Ophthalmol Vis Sci. 2009; 50:441–451. [PubMed: 18676633]
22. Stitt AW, Hughes SJ, Canning P, Lynch O, Cox O, Frizzell N, Thorpe SR, Cotter TG, Curtis TM, Gardiner TA. Substrates modified by advanced glycation end-products cause dysfunction and death in retinal pericytes by reducing survival signals mediated by platelet-derived growth factor. Diabetologia. 2004; 47:1735–1746. [PubMed: 15502926]
23. Finnegan S, Robson JL, Wylie M, Healy A, Stitt AW, Curry WJ. Protein expression profiling during chick retinal maturation: a proteomics-based approach. Proteome Sci. 2008; 6:34. [PubMed: 19077203]
24. McKay GJ, Campbell L, Oliver M, Brockbank S, Simpson DA, Curry WJ. Preparation of planar retinal specimens: verification by histology, mRNA profiling, and proteome analysis. Mol Vis. 2004; 10:240–247. [PubMed: 15064678]
25. West KA, Yan L, Shadrach K, Sun J, Hasan A, Miyagi M, Crabb JS, Hollyfield JG, Marmorstein AD, Crabb JW. Protein database, human retinal pigment epithelium. Mol Cell Proteomics. 2003; 2:37–49. [PubMed: 12601081]
26. Alge CS, Hauck SM, Priglinger SG, Kampik A, Ueffing M. Differential protein profiling of primary versus immortalized human RPE cells identifies expression patterns associated with cytoskeletal remodeling and cell survival. J Proteome Res. 2006; 5:862–878. [PubMed: 16602694]
27. An E, Lu X, Flippin J, Devaney JM, Halligan B, Hoffman EP, Strunnikova N, Csaky K, Hathout Y. Secreted proteome profiling in human RPE cell cultures derived from donors with age related macular degeneration and age matched healthy donors. J Proteome Res. 2006; 5:2599–2610. [PubMed: 17022631]

28. Nordgaard CL, Berg KM, Kapphahn RJ, Reilly C, Feng X, Olsen TW, Ferrington DA. Proteomics of the retinal pigment epithelium reveals altered protein expression at progressive stages of age-related macular degeneration. Invest Ophthalmol Vis Sci. 2006; 47:815–822. [PubMed: 16505012]
29. Warburton S, Southwick K, Hardman RM, Secrest AM, Grow RK, Xin H, Woolley AT, Burton GF, Thulin CD. Examining the proteins of functional retinal lipofuscin using proteomic analysis as a guide for understanding its origin. Mol Vis. 2005; 11:1122–1134. [PubMed: 16379024]
30. Warburton S, Davis WE, Southwick K, Xin H, Woolley AT, Burton GF, Thulin CD. Proteomic and phototoxic characterization of melanolipofuscin: correlation to disease and model for its origin. Mol Vis. 2007; 13:318–329. [PubMed: 17392682]
31. Shibuya M, Okamoto H, Nozawa T, Utsumi J, Reddy VN, Echizen H, Tanaka Y, Iwata T. Proteomic and transcriptomic analyses of retinal pigment epithelial cells exposed to REF-1/TFPI-2. Invest Ophthalmol Vis Sci. 2007; 48:516–521. [PubMed: 17251444]
32. Yokoyama T, Yamane K, Minamoto A, Tsukamoto H, Yamashita H, Izumi S, Hoppe G, Sears JE, Mishima HK. High glucose concentration induces elevated expression of anti-oxidant and proteolytic enzymes in cultured human retinal pigment epithelial cells. Exp Eye Res. 2006; 83:602–609. [PubMed: 16697369]
33. Alge CS, Suppmann S, Priglinger SG, Neubauer AS, May CA, Hauck S, Welge-Lussen U, Ueffing M, Kampik A. Comparative proteome analysis of native differentiated and cultured dedifferentiated human RPE cells. Invest Ophthalmol Vis Sci. 2003; 44:3629–3641. [PubMed: 12882817]
34. Schutt F, Ueberle B, Schnolzer M, Holz FG, Kopitz J. Proteome analysis of lipofuscin in human retinal pigment epithelial cells. FEBS Lett. 2002; 528:217–221. [PubMed: 12297308]
35. Guidry C, Medeiros NE, Curcio CA. Phenotypic variation of retinal pigment epithelium in age-related macular degeneration. Invest Ophthalmol Vis Sci. 2002; 43:267–273. [PubMed: 11773041]
36. Kueper T, Grune T, Prahl S, Lenz H, Welge V, Biernoth T, Vogt Y, Muhr GM, Gaemlich A, Jung T, Boemke G, Elsasser HP, Wittern KP, Wenck H, Stab F, Blatt T. Vimentin is the specific target in skin glycation. Structural prerequisites, functional consequences, and role in skin aging. J Biol Chem. 2007; 282:23427–23436. [PubMed: 17567584]
37. Obin M, Lee BY, Meinke G, Bohm A, Lee RH, Gaudet R, Hopp JA, Arshavsky VY, Willardson BM, Taylor A. Ubiquitylation of the transducin betagamma subunit complex. Regulation by phosducin. J biol Chem. 2002; 277:44566–44575. [PubMed: 12215439]
38. Wagner M, Benson MT, Rennie IG, MacNeil S. Effects of pharmacological modulation of intracellular signalling systems on retinal pigment epithelial cell attachment to extracellular matrix proteins. Curr Eye Res. 1995; 14:373–384. [PubMed: 7648863]
39. Smith-Thomas L, Haycock JW, Metcalfe R, Boulton M, Ellis S, Rennie IG, Richardson PS, Palmer I, Parsons MA, Mac Neil S. Involvement of calcium in retinal pigment epithelial cell proliferation and pigmentation. Curr Eye Res. 1998; 17:813–822. [PubMed: 9723997]
40. Graven KK, Molvar C, Roncarati JS, Klahn BD, Lowrey S, Farber HW. Identification of protein disulfide isomerase as an endothelial hypoxic stress protein. Am J Physiol. 2002; 282:L996–L1003.
41. Honda S, Farboud B, Hjelmeland LM, Handa JT. Induction of an aging mRNA retinal pigment epithelial cell phenotype by matrix-containing advanced glycation end products in vitro. Investig Ophthalmol Vis Sci. 2001; 42:2419–2425. [PubMed: 11527959]
42. Yaung J, Jin M, Barron E, Spee C, Wawrousek EF, Kannan R, Hinton DR. alpha-Crystallin distribution in retinal pigment epithelium and effect of gene knockouts on sensitivity to oxidative stress. Mol Vis. 2007; 13:566–577. [PubMed: 17438522]
43. Chen YS, Hackett SF, Schoenfeld CL, Vinores MA, Vinores SA, Campochiaro PA. Localisation of vascular endothelial growth factor and its receptors to cells of vascular and avascular epiretinal membranes. Br J Ophthalmol. 1997; 81:919–926. [PubMed: 9486038]
44. Puig A, Gilbert HF. Protein disulfide isomerase exhibits chaperone and anti-chaperone activity in the oxidative refolding of lysozyme. J Biol Chem. 1994; 269:7764–7771. [PubMed: 7907332]
45. Tanaka S, Uehara T, Nomura Y. Up-regulation of protein-disulfide isomerase in response to hypoxia/brain ischemia and its protective effect against apoptotic cell death. J Biol Chem. 2000; 275:10388–10393. [PubMed: 10744727]

46. Ko HS, Uehara T, Nomura Y. Role of ubiquilin associated with protein-disulfide isomerase in the endoplasmic reticulum in stress-induced apoptotic cell death. J Biol Chem. 2002; 277:35386–35392. [PubMed: 12095988]
47. Decanini A, Nordgaard CL, Feng X, Ferrington DA, Olsen TW. Changes in select redox proteins of the retinal pigment epithelium in age-related macular degeneration. Am J Ophthalmol. 2007; 143:607–615. [PubMed: 17280640]
48. Taraseviciene-Stewart L, Kasahara Y, Alger L, Hirth P, Mc Mahon G, Waltenberger J, Voelkel NF, Tuder RM. Inhibition of the VEGF receptor 2 combined with chronic hypoxia causes cell death-dependent pulmonary endothelial cell proliferation and severe pulmonary hypertension. FASEB J. 2001; 15:427–438. [PubMed: 11156958]
49. Garrido R, Mattson MP, Hennig B, Toborek M. Nicotine protects against arachidonic-acid-induced caspase activation, cytochrome c release and apoptosis of cultured spinal cord neurons. J Neurochem. 2001; 76:1395–1403. [PubMed: 11238724]
50. Hochstrasser M. Ubiquitin-dependent protein degradation. Annu Rev Genet. 1996; 30:405–439. [PubMed: 8982460]
51. Lowe J, McDermott H, Landon M, Mayer RJ, Wilkinson KD. Ubiquitin carboxyl-terminal hydrolase (PGP 9.5) is selectively present in ubiquitinated inclusion bodies characteristic of human neurodegenerative diseases. J Pathol. 1990; 161:153–160. [PubMed: 2166150]
52. Nishikawa K, Li H, Kawamura R, Osaka H, Wang YL, Hara Y, Hirokawa T, Manago Y, Amano T, Noda M, Aoki S, Wada K. Alterations of structure and hydrolase activity of parkinsonism-associated human ubiquitin carboxyl-terminal hydrolase L1 variants. Biochem Biophys Res Commun. 2003; 304:176–183. [PubMed: 12705903]
53. Kurihara LJ, Kikuchi T, Wada K, Tilghman SM. Loss of Uch-L1 and Uch-L3 leads to neurodegeneration, posterior paralysis and dysphagia. Hum Mol Genet. 2001; 10:1963–1970. [PubMed: 11555633]
54. Esteve-Rudd J, Campello L, Herrero MT, Cuenca N, Martin-Nieto J. Expression in the mammalian retina of parkin and UCH-L1, two components of the ubiquitin-proteasome system. Brain Res. 2010; 1352:70–82. [PubMed: 20638372]
55. Loeffler KU, Mangini NJ. Immunolocalization of ubiquitin and related enzymes in human retina and retinal pigment epithelium. Graefes Arch Clin Exp Ophthalmol. 1997; 235:248–254. [PubMed: 9143894]
56. Xu H, Chen M, Manivannan A, Lois N, Forrester JV. Age-dependent accumulation of lipofuscin in perivascular and sub-retinal microglia in experimental mice. Aging Cell. 2008; 7:58–68. [PubMed: 17988243]
57. Crabb JW, Miyagi M, Gu X, Shadrach K, West KA, Sakaguchi H, Kamei M, Hasan A, Yan L, Rayborn ME, Salomon RG, Hollyfield JG. Drusen proteome analysis: an approach to the etiology of age-related macular degeneration. Proc Natl Acad Sci U S A. 2002; 99:14682–14687. [PubMed: 12391305]

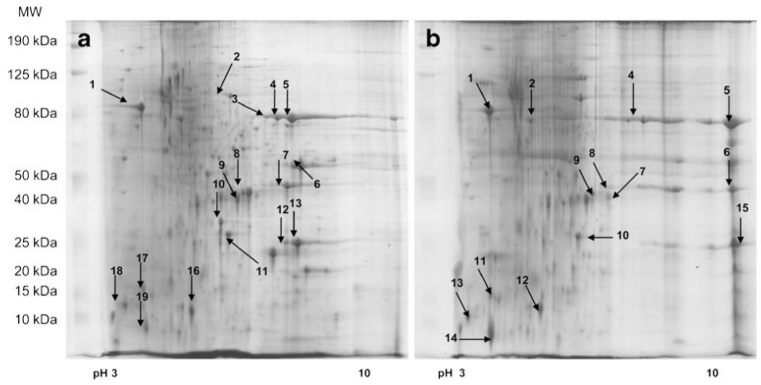

Fig. 1.

Representative 2-dimensional gel electrophoresis (2D) profiles of the ARPE-19 proteome derived from cells cultured on unmodified matrix (BM) (**a**) and AGE-modified matrices (AGE-BM) (**b**); 2 mg of the protein extract was separated by IEF (pH gradient 3–10 IPG strips), arrayed on12.5% gels, visualized using colloidal Coomassie Blue, and subjected to densitometry. Spots of interest (*annotated*) were identified by LC ESI–MS/MS (Table 1)

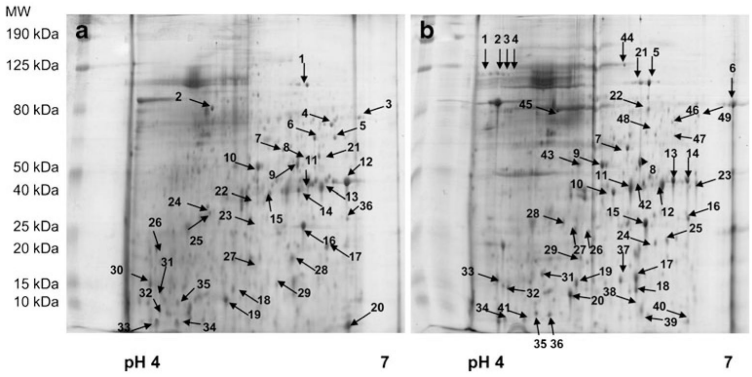

Fig. 2.

Representative 2-dimensional gel electrophoresis (2DGE) profiles of the ARPE-19 proteome cultured on (**a**) unmodified BM and (**b**) AGE-BM; 2 mg of the protein extract was separated by IEF (pH gradient 4–7 IPG strips), arrayed on 12.5% gels, visualized using colloidal Coomassie Blue, and subjected to densitometry. Spots of interest (*annotated*) were identified by LC ESI–MS/MS (Table 1)

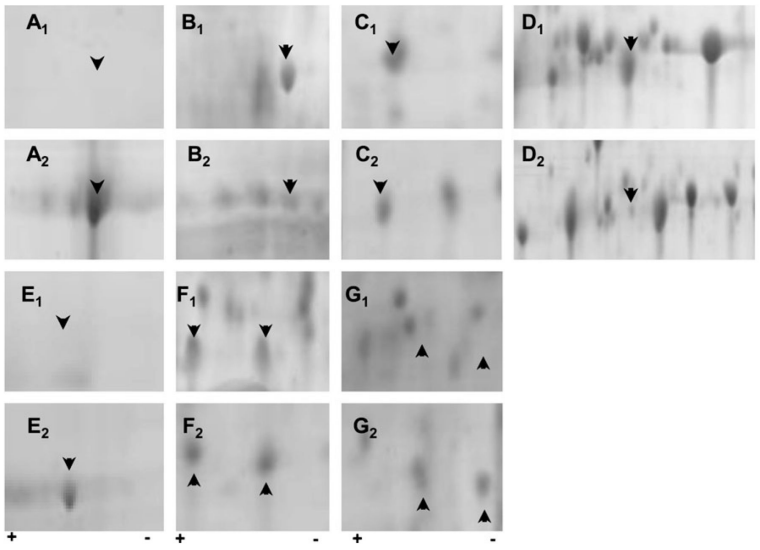

Fig. 3.

Posttranslational modifications evident in ARPE19 monolayers exposed to either unmodified matrix (BM) (**a1**-**g1**) or glycation (AGE-BM) (**a2**-**g2**). The most significantly altered 2D regions are highlighted for protein alterations occurring with and without matrix modification. *Arrowheads* indicate proteins of interest correlating with a selection of data in Table 1. Identified proteins include **a**: α enolase phospho D glycerate (47 kDa); **b**: vimentin (53.5 kDa); **c**: nucleoside diphosphate kinase A (17.1 kDa); **d**: heat shock protein beta1 (22.8 kDa); **e**: stress-70 protein (73.6 kDa); **f**: barrier to auto-integration factor (10 kDa) nuclear transport factor 2 (14.5 kDa); **g**: peroxiredoxin 2 (21.9 kDa); lactoylglutathione lyase (20.6 kDa)

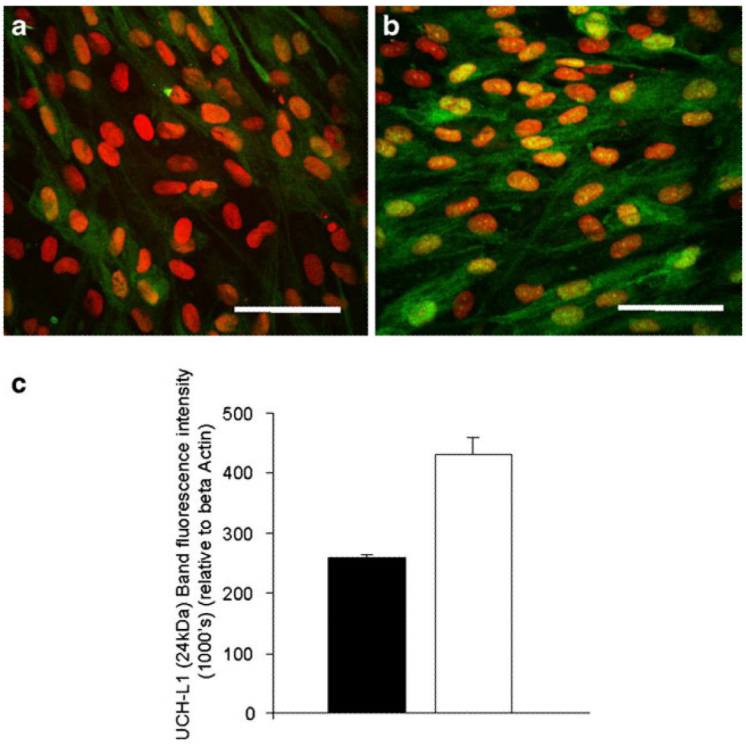

Fig. 4.

Upregulation of UCH-L1 within confluent ARPE19 monolayers grown on AGE-BM. **a** Control ARPE-19 growing on native BM show sparse UCH-L1 immunoreactivity (*green*); control cells grown on AGE-BM (**b**) display a relative increase in the cytoplasmic intensity. Nuclei are counterstained with PI (*red*). *Scale bar* — 50 μm. **c** Western blot analysis using fluorescence detection of the 24 kDa UCHL-1 band quantified using LI-COR and expressed relative to β-actin expression (n=3)

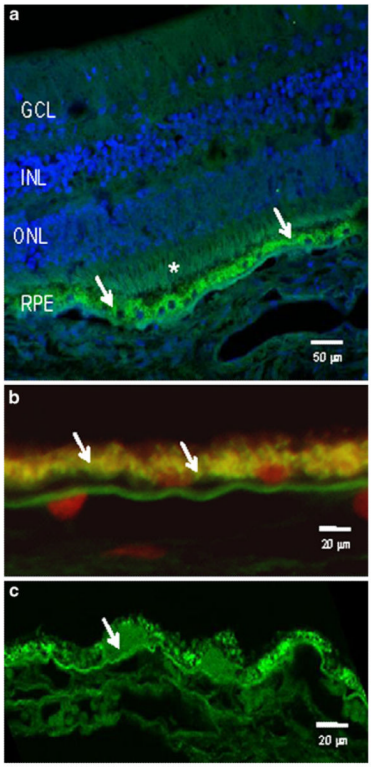

Fig. 5.

UCH-L1 in human retina. **a** Representative image from a male donor aged 34 years in which UCHL-1 immunoreactivity is evident at the photoreceptors (*) and, in particular at the RPE (*arrows*). **b** Higher magnification of RPE from a young donor (aged 30–40) showing UCH-L1 at the basal face of the cells (*arrows*), adjacent to Bruch's membrane. Nuclei are counterstained with propidium iodide (*red*). **c** An 88-year-old donor demonstrated intense UCH-L1 immunostaining in the RPE cytoplasm and in drusen (*arrows*)

Table 1

2D arrayed proteins identified by LC ESI MS/MS

Protein	Accession number[a]	2D unmodified gel spot number[b]	2D AGE BM gel spot number[c]	Score	Coverage (%)	Calculated molecular mass (Da)[d]	PI [d]	Fold change to control matrix (*n*=3)	Up/down regulation	Previously identified ref. no.
Protein disulphide isomerase	P30101	1	5	11.6	30.7	56746	5.98	2.08	U	
Gamma enolase	P09104	2	45	11.6	58.2	47108	4.91	0.96	N	25 -
Phosphoglycerate kinase	P00558	4	46	11.6	44.8	44568	8.52	8.37	D	25 -
c myc promoter binding protein	P22712	5	47	11.6	11.0	37063	7.23	4.86	D	25 -
c myc promoter binding protein	P22712	6	48	11.6	11.0	37063	7.23	4.14	D	25 -
Cathepsin D precursor	P07339	3	8	11.6	2.2	44523	6.1	1.30	N	25 26
Cathepsin D precursor	P07339	10	9	11.6	10.9	44523	6.1	0.71	N	25 26
Triosephosphate isomerase	P60174	12	14	11.6	63.7	26521	6.51	2.64	D	–26
Heat shock protein beta-1	P04792	14	42	11.6	9.3	22768	5.98	2.11	D	25 -
Ubiquitin carboxyl-terminal hydrolase 1	P09936	15	10	11.6	17.5	24808	5.33	4.54	U	–
Superoxide dismutase	P00441	16	15			15794	5.7	0.92	N	–26
Galectin 1	P09382	19	20	11.6	72.4	14575	5.34	0.89	N	–26
Tumour necrosis factor b prescursor	P01375	20	40	11.6	24.9	25628	6.88	5.91	D	–
Nucleophosmin	P06748	26	30			32555	4.64	1.67	N	–26
14 kDa phosphohistidine phosphatase	Q9NRX4	29	37			13824	5.65	1.01	N	–
Myosin light polypeptide 6	P60660	30	33			16788	4.56	1.13	N	–
Myosin light polypeptide 6	P60660	31	32			16788	4.56	1.29	N	–
Aminoacylase-1	Q03154	35	22			45856	5.77	0.74	N	–
Thioredoxin dependent peroxide	P30048	36	16	9.9	14.1	27675	8.09	1.91	N	25 26
Calreticulin precursor, CRP55 [f]	P27797	1	1	11.6	3.0	48112	4.29	1.28	N	25 -
Glutathione peroxidase [f]	P07203	18	17			21885	6.50	1.16	N	–
Galectin 1 [f]	P09382	23	19	11.6	72.4	14575	5.38	1.41	N	–26
Myosin regulatory light chain [f]	P19105	24	18			19650	4.66	1.53	N	–

Graefes Arch Clin Exp Ophthalmol. Author manuscript; available in PMC 2013 June 05.

Protein	Accession number[a]	2D unmodified gel spot number[b]	2D AGE BM gel spot number[c]	Score	Coverage (%)	Calculated molecular mass (Da)[d]	pI [d]	Fold change to control matrix (*n*=3)	Up/down regulation	Previously identified ref. no.
Calmodulin [f]	P02593	25	20	10.5	23.6	16695	4.08	2.94	U	–
Proactivator polypeptide precursor [f]	P07602	26	21	11.6	5.3	58073	5.12	3.56	U	–

[a] Accession numbers can be accessed through NCBI. To access use the link http://www.ncbi.nlm.nih.gov:80/entrez.query.fcgi?db=Protein

[b] Representative 2DPAGE profiles for these spots are shown in Fig. 1

[c] Representative 2DPAGE profiles for these spots are shown in Fig. 2

[d] Spot data was calculated from spots excised from gels focused at both wide range (pH 3–10) & narrow range (pH 4–7) IEF

[e] This alteration is relative to proteins identified by ESI-MS/MS from ARPE-19 cells exposed to an unmodified matrix and an AGE-modified matrix, with values normalized to control gels. U: significantly upregulated; D: significantly downregulated; N: no significant fold change

[f] These proteins are taken from ARPE-19 cells exposed to unmodified MG and AGE-BM matrices for 1 month

All samples are from a homo sapiens source

Table 2

Functional categories of the 55 proteins identified by ESI-MS/MS; the largest percentages were cytoskeletal, antioxidant, metabolic, UPP, and heat shock protein

Functional categories	% contribution
Cytoskeleton proteins	17
Heat shock proteins + chaperones	17
Metabolism	15
Miscellaneous	13
RNA binding proteins, elongation and transcription related	10
Apoptosis-related proteins	8
Antioxidants	8
Ubiquitination + proteasome-related proteins	8
Signalling proteins	4